

is an overestimate, since adsorption occurs when the molecules strike the surface. (Such an adsorption would imply a partial exhaustion of the solution in the vicinity of the crystal and a decrease of the flux of molecules incident to the growth facet.) Moreover, the calculation is for the number of molecules that hit the surface and not for the number of molecules that are adsorbed and diffused to the growth step in a very short time. The apparent agreement claimed by Hoffman between the predicted and experimental values of  $G$  relies on the introduction of various arbitrary parameters in the expression of  $G$ . More particularly, one may notice  $C_0$  and the empirical concentration factor  $c^{0.4}$ , which cannot have physical meaning because it depends on the units in which  $c$  is expressed. For the sake of completeness, we observe with Hoffman<sup>3</sup> that origin and estimation of  $C_0$  are challenges that still confront his theory, and we examine thus the effect of other choices for  $C_0$  and  $L_p$ .

In the picture given by Hoffman the area of a nucleation site for a full stem is very small ( $1.2 \times 10^{-17} \text{ cm}^2$ ). Accordingly, Hoffman accepts that  $C_0$  may have lower values. But the effect of choosing  $C_0 < 10^4$  is to increase the value of  $g$  (eq 1 and 3). Similarly, choice of a lower value of  $L_p$  leads to an increase of calculated value for  $g$  (eq 2 and 3). As an example, if we choose  $C_0 = 10^2$ ,  $\sigma(1 - \gamma) = 9.42 \text{ erg/cm}^2$ , and  $L_p \leq 10^{-4} \text{ cm}$ , we get  $G_{\text{calcd}} \leq G_{\text{exptl}}$ ,  $L_k > 0.47 \text{ cm}$ ,  $g > 3.32 \times 10^3 \text{ cm/s}$ , and  $A_n = 1.2 \times 10^{-15} \text{ cm}^2$ . The values of  $g$  and  $A_n$  are again too large and too small, respectively.

We examine now the origin and significance of these incorrect predictions. The incoherence comes from overestimation of  $(2g/i)^{1/2}$ , which is a direct consequence of the occurrence of the factor  $\exp(2b\sigma(1-\gamma)l_x/kT)$  on the right-hand side of eq 1. This factor represents the effect of the large free energy barrier associated with the deposition of a full first stem. As shown in our paper with Kovacs,<sup>1</sup> the barrier may be lowered *fictitiously* by assuming *formally* low values of  $\sigma$ , but far too low to be credible. The way to escape this paradox has previously been given:<sup>9,10</sup> the nucleus must be assumed to build up piecemeal by successive addition of parts of the first stem. In this way we get a free energy barrier expressed by  $2b\sigma\Delta l$ , in which  $\Delta l$  is much smaller than  $l_x(1 - \gamma)$ . From my point of view<sup>1,2,8</sup> the same basic objection may be formulated as a concern in the application of the H-L theory to growth of folded-chain crystals.

Two very simple criteria have been used throughout this work and are of general applicability: (i) If the growth rate does not increase with the crystal size,  $L_p$ ,  $L_k$ , or both are smaller than the crystal size. In most cases this leads to the conclusion that only the polynucleation regime is plausible. (ii) The estimation of the order of magnitude of both  $g$  and  $A_n$  is very illuminating. Often this simple calculation rules out the applicability of the H-L kinetic theory of crystal growth unless the nucleation term is modified as explained above. If this modification is made, the limitation of the thickness of folded-chain crystals does not result from a free energy balance pertaining to a full fold length.<sup>9</sup>

**Acknowledgment.** We thank Prof. A. J. Kovacs for helpful comments and the Fonds National de la Recherche Scientifique (Belgium) for partial support.

**Registry No.** Polyethylene (homopolymer), 9002-88-4.

## References and Notes

- (1) Point, J. J.; Kovacs, A. J. *Macromolecules* **1980**, *13*, 399.
- (2) Point, J. J. *Discuss. Faraday Soc.* **1979**, *68*, 167.
- (3) Hoffman, J. D. *Macromolecules* **1985**, *18*, 772.
- (4) Frank, F. C. *J. Cryst. Growth* **1971**, *22*, 233.
- (5) (a) Leung, W. M.; Manley, R. St. J.; Panaras, A. R. *Macromolecules* **1985**, *18*, 760. (b) Manley, R. St. J., personal communication.
- (6) Hoffman, J. D.; Davis, G. T.; Lauritzen, J. I., Jr. In "Treatise on Solid State Chemistry"; Hannay, N. B., Ed.; Plenum Press, New York.
- (7) When crystallization occurs from the melt, a large value of  $g$  may be plausible according to Hoffman (private communication).
- (8) Point, J. J.; Colet, M. C.; Dosiere, M. J. *Polym. Sci.*, submitted.
- (9) Point, J. J. *Macromolecules* **1979**, *12*, 770.
- (10) DiMarzio, E. A.; Guttman, C. M. *J. Appl. Phys.* **1982**, *53*, 6581.
- (11) Simon, B.; Grassi, A.; Boistelle, R. *J. Cryst. Growth* **1974**, *26*, 77.

J. J. Point

Université de l'Etat à Mons  
7000-Mons, Belgium

Received June 10, 1985

## CP/MAS <sup>13</sup>C NMR Spectroscopy of Hydrated Amyloses Using a Magic-Angle Spinning Rotor with an O-Ring Seal

Many kinds of synthetic and naturally occurring polymers have been examined by cross-polarization/magic-angle sample spinning (CP/MAS) <sup>13</sup>C NMR spectroscopy. However, most of these measurements have been performed in the dry state and only a few reports<sup>1-3</sup> have been published on polymers containing some water. A major obstacle in the application of this form of spectroscopy to such hydrated polymers is that the large centrifugal force produced by rapid spinning readily removes water from samples packed in a conventional MAS rotor. We have recently developed a new rotor with an O-ring seal by modifying a commercial bullet-type rotor. This type of rotor can be steadily rotated at a rate of 3-4 kHz without practical loss of water for samples with any water content. Its high performance is sufficiently good, even for 1-week measurements, that <sup>13</sup>C spin-lattice relaxation times,  $T_1$ , which are normally of the order of 10-1000 s for crystalline components of polymers, can also be obtained.

In this communication we report CP/MAS <sup>13</sup>C NMR studies of corn and potato starches with different water contents. These two samples have different crystalline forms defined as A- and B-amyloses, respectively, which are assumed to be identical in molecular conformation but to differ with respect to the packing of the helical chains.<sup>4,5</sup> In addition, water molecules are arranged in different ways for the two forms. Therefore, CP/MAS <sup>13</sup>C NMR measurements in hydrated forms are essential for those samples to characterize the detailed molecular conformation and chain dynamics.

The MAS rotor shown in Figure 1 was machined from poly(chlorotrifluoroethylene), Daifuron (Daikin Co. Ltd.), which was annealed in advance at temperatures above 195 °C. This sort of annealing was necessary to improve the long-term stability of the spinning. An O-ring made of nitrile rubber with carbon black was used, since there was no appreciable contribution from this material in the spectra. CP/MAS <sup>13</sup>C NMR measurements were carried out with a JEOL JNM-FX200 spectrometer equipped with a CP/MAS unit operating under a static magnetic field of 4.7 T. The spinning rate was 3.2-3.5 kHz for both dry and hydrated samples. <sup>1</sup>H and <sup>13</sup>C radiofrequency field strengths  $\gamma B_1/2\pi$  were 69 kHz for the CP process, while the <sup>1</sup>H dipolar decoupling field was set to 54 kHz. The contact time was 2.0 ms throughout this work. The chemical shifts relative to tetramethylsilane (Me<sub>4</sub>Si) were

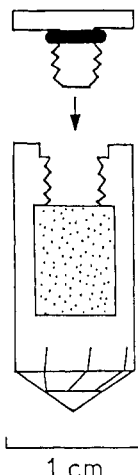


Figure 1. Schematic diagram of a MAS rotor with an O-ring seal.

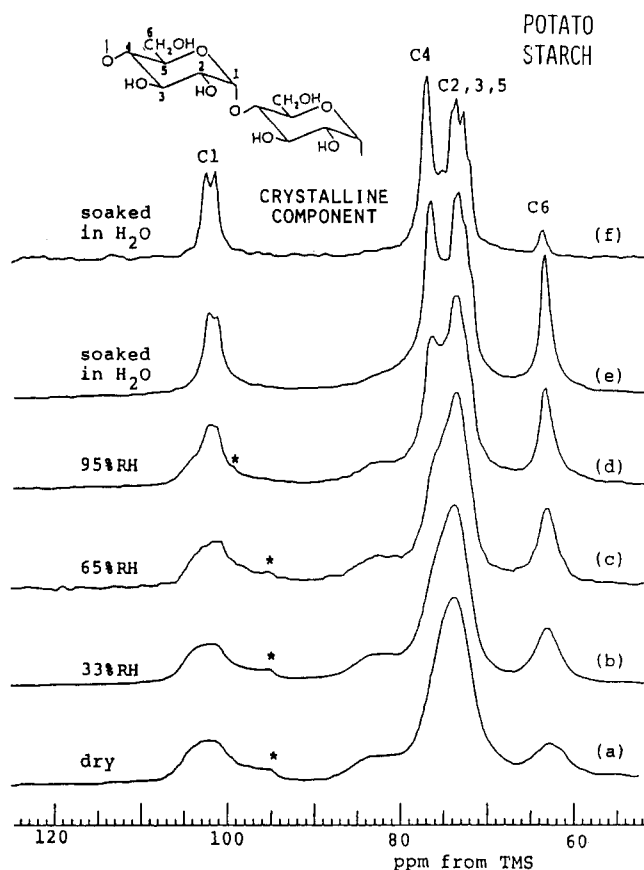


Figure 2. 50-MHz CP/MAS  $^{13}\text{C}$  NMR spectra of potato starch with different water contents: (a) 0%; (b) 11.1%; (c) 20.1%; (d) 32.3%; (e); (f) 101%. The asterisk designates a spinning sideband from polyethylene inserted in each sample as an internal reference.

determined by using the crystalline peak at 33.6 ppm of polyethylene as an internal standard.

Commercial corn and potato starches in powder form were purified by Soxhlet extraction with methanol. Water contents,  $(\text{g of H}_2\text{O/g of amylose}) \times 100$ , were adjusted by exposing the samples to atmospheres of different relative humidities (RH) or by soaking them in deionized water.

Figure 2 shows 50-MHz CP/MAS  $^{13}\text{C}$  NMR spectra of potato starch with different water contents as measured with the rotor shown in Figure 1. The spectrum of the crystalline component (B-amylose) is shown in Figure 2f, which was recorded as a longer  $T_1$  component of the sample with the use of Torchia's pulse sequence<sup>6</sup>, as described later. Each resonance line of the dry sample is very broad

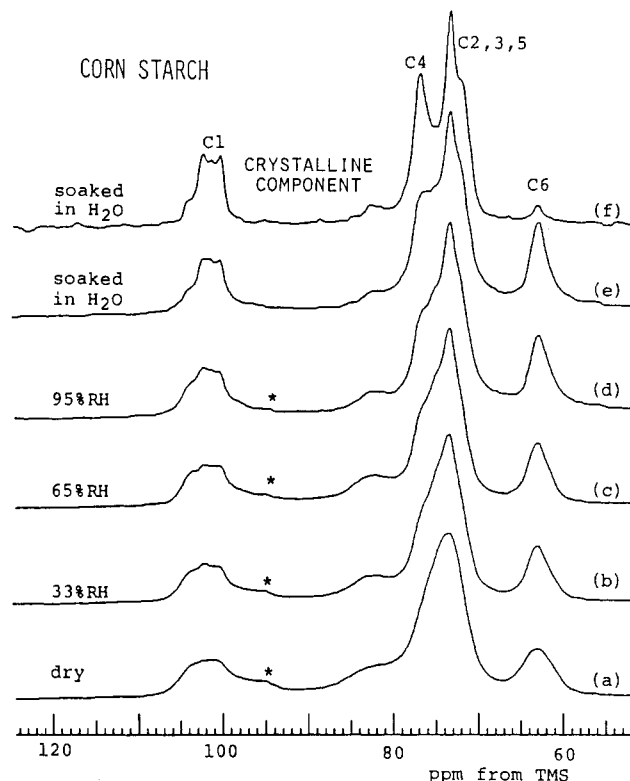


Figure 3. 50-MHz CP/MAS  $^{13}\text{C}$  NMR spectra of corn starch with different water contents: (a) 0%; (b) 11.0%; (c) 17.7%; (d) 27.9%; (e); (f) 100%.

and almost structureless, as frequently observed for non-crystalline polymers. Such broadness is caused mainly by the spread in isotropic chemical shifts due to the non-equivalences in chain conformation and packing. However, the lines narrow markedly with increasing water content, resulting in the appearance of the fine splitting to the C1 line. In addition, the sharp C4 line can be clearly observed at 76.3 ppm, although the upfield broad C4 line at about 82.5 ppm decreases in intensity. These features can be better recognized in the crystalline spectrum in Figure 2f, where we also show the assignments of the respective carbons made by analogy with the solution-state spectrum.<sup>7,8</sup> According to our results,<sup>9,10</sup> the chemical shift of 62.7 ppm of the C6 carbon corresponds to the gauche-trans conformation of the  $\text{CH}_2\text{OH}$  group, which is in good agreement with the result of X-ray analysis.<sup>4</sup>

Similar spectra have been obtained for corn starch, as shown in Figure 3. The chemical shift and the line shape of each resonance are almost the same as those of potato starch in the dry state. However, the differences in the spectra of the two samples become clear with increasing water content; the C1 line appears to split into a triplet in corn starch under the resolution of the spectrometer<sup>11</sup> while it splits into a doublet in potato starch. It is difficult to assign the cause of the difference in the splitting mode between the two samples at present, because the origin of similar splittings observed in different polymorphs of cellulose is still unknown.<sup>9,12-15</sup> One possible interpretation may be made in terms of the difference in packing of helical chains in the unit cells of A- and B-amyloses. In these cases no small conformational difference is likely to cause the splittings because such differences should be averaged out by enhanced torsional motions about the  $\alpha$ -1,4-glycosidic linkages, as will be described below. On the other hand, the orientation of the  $\text{CH}_2\text{OH}$  group in A-amylose has not been unambiguously determined by X-ray analysis; it may be either all gauche-trans or a

**Table I**  
 **$^{13}\text{C}$  Spin-Lattice Relaxation Times  $T_{1C}$  of the Carbons of Amylose**

	water content, <sup>a</sup> %	$T_1$ /s			
		C1	C4	C2,3,5	C6
A-amylose	0	20.3	17.6	16.3	3.7
	100	8.9	6.6	5.1	1.6
B-amylose	0	21.0	18.3	16.1	3.0
	101	8.7	8.9	7.5	1.9

<sup>a</sup> (g of water)/(g of polymer)  $\times$  100.

mixture of gauche-trans and trans-gauche.<sup>5</sup> However, it can be concluded from the chemical shift (62.7 ppm) of the C6 carbon that the  $\text{CH}_2\text{OH}$  group of A-amylose adopts the gauche-trans conformation.<sup>9,10</sup>

Table I lists  $^{13}\text{C}$   $T_1$  values of A- and B-amyloses measured by Torchia's pulse sequence.<sup>6</sup> Although each line has at least two components with different  $T_1$ 's, longer  $T_1$ 's are assumed to be the values of the crystalline component. The  $T_1$  values of the pyranose ring carbons are of the order of 5-9 s for the hydrated A- and B-amyloses, whereas the values are significantly longer in the dry state. Almost the same effect of hydration on  $T_1$  values was observed in the case of the samples soaked in  $\text{D}_2\text{O}$ . It is therefore concluded that water enhances the torsional motion about the  $\alpha$ -1,4-glycosidic linkage even in the crystalline region. Such high molecular mobility of the amylose chains may stem from the flexibility of the sixfold structure.<sup>4,5</sup> In contrast, cellulose molecules containing  $\beta$ -1,4-glycosidic linkages adopt the twofold helical structure, which is an almost linear conformation without flexibility.<sup>16-19</sup> This rigid structure will be reflected in much longer  $T_1$  values obtained for different cellulose samples in both dry and hydrated forms.<sup>3,9,20</sup>

The  $T_1$ 's of the C6 carbons of the two polymorphs of amylose are shorter than those of the ring carbons in both the dry and hydrated forms, indicating that the  $\text{CH}_2\text{OH}$  groups undergo enhanced torsional motion about the exocyclic C5-C6 bond. This is also in contrast to the result<sup>3,9,20</sup> of cellulose crystals; the  $T_1$  values of their C6 carbons are of almost the same order as those of their ring carbons, suggesting hindrance of the torsional motion about the C5-C6 bond. Such a difference in the torsional mobility of the  $\text{CH}_2\text{OH}$  groups between amylose and cellulose may be related to the difference in hydrogen bonding. In A- and B-amyloses most of the hydrogen bonds are formed along the helical chain<sup>4,5</sup> and thus the mobility of  $\text{CH}_2\text{OH}$  groups is also closely associated with the high flexibility of the helical chains. On the other hand, all  $\text{CH}_2\text{OH}$  groups are fixed by inter- and intrachain hydrogen bonding in cellulose I and II<sup>16-19</sup> and furthermore the main chains are also very limited in molecular mobility.<sup>20</sup> More detailed analysis of molecular chain conformation and dynamics will be published elsewhere for regenerated samples in the A, B, and V forms.

## References and Notes

- (1) VanderHart, D. L. National Bureau of Standards Report NBSIR 82-2834, 1982.
- (2) Fyfe, C. A.; Stephenson, P. J.; Taylor, M. G.; Bluhm, T. L.; Deslandes, Y.; Marchessault, R. H. *Macromolecules* **1984**, *17*, 501.
- (3) Horii, F.; Hirai, A.; Kitamaru, R.; Sakurada, I. *Cellulose Chem. Technol.* **1985**, *19*, 513.
- (4) Wu, H.-C.H.; Sarko, A. *Carbohydr. Res.* **1978**, *61*, 7.
- (5) Wu, H.-C.H.; Sarko, A. *Carbohydr. Res.* **1978**, *62*, 27.
- (6) Torchia, D. A.; *J. Magn. Reson.* **1978**, *30*, 613.
- (7) Colson, P.; Jenning, H. J.; Smith, I. C. P. *J. Am. Chem. Soc.* **1974**, *96*, 8081.
- (8) Friebolin, H.; Frank, N.; Keilich, G.; Siefert, E. *Makromol. Chem.* **1976**, *177*, 845.

- (9) Horii, F.; Hirai, A.; Kitamaru, R. "Polymers for Fibers and Elastomers"; Arthur, J. C., Jr., Ed.; American Chemical Society: Washington, DC, 1984; ACS Symp. Ser. No. 260, p 27.
- (10) Horii, F.; Hirai, A.; Kitamaru, R. *Polym. Bull.* **1983**, *10*, 357.
- (11) The origin of the downfield shoulder of the C1 line and the small peak of the C4 carbon near 82.5 ppm in Figure 3f is not clear at present. However, it should be noted that the  $^{13}\text{C}$  chemical shifts of these components are in good accord with those of the  $V_h$  form of the regenerated amylose.
- (12) Atalla, R. H.; Gast, J. C.; Sindorf, D. W.; Bartuska, V. J.; Maciel, G. E. *J. Am. Chem. Soc.* **1980**, *102*, 3249.
- (13) Horii, F.; Hirai, A.; Kitamaru, R. *Polym. Bull.* **1982**, *8*, 163.
- (14) VanderHart, D. L.; Atalla, R. H. *Macromolecules* **1984**, *17*, 1465.
- (15) Cael, J. J.; Kwok, D. L. W.; Bhattacharjee, S. S.; Patt, S. L. *Macromolecules* **1985**, *18*, 821.
- (16) Gardner, K. H.; Blackwell, J. *Biopolymers* **1974**, *13*, 1975.
- (17) Kolpak, K. J.; Blackwell, J. *Macromolecules* **1976**, *9*, 273.
- (18) Woodcock, C.; Sarko, A. *Macromolecules* **1980**, *13*, 1183.
- (19) Stipanovic, A. J.; Sarko, A. *Macromolecules* **1976**, *9*, 851.
- (20) Horii, F.; Hirai, A.; Kitamaru, R. *J. Carbohydr. Chem.* **1984**, *3*, 641.

F. Horii,\* A. Hirai, and R. Kitamaru

Institute for Chemical Research  
Kyoto University, Uji, Kyoto 611, Japan

Received August 6, 1985

## Nonideal Mixing in Binary Blends of Perdeuterated and Protonated Polystyrenes

Recently, we demonstrated<sup>1</sup> that amorphous mixtures of normal (protonated) and perdeuterated 1,4-polybutadienes are characterized by an upper critical solution temperature (UCST), contradicting the widely held assumption that such isotopic mixtures form ideal solutions. This effect was shown<sup>1</sup> to derive from a small difference in segment volume between the perdeuterated and normal species, as predicted by Buckingham and Hentschel.<sup>2</sup> In the symmetric case ( $N_D = N_H = N$ ), the predicted critical degree of polymerization for amorphous isotopic polymer mixtures is

$$N_c = 4k_B T_c / V(\Delta V/V)^2 \quad (1)$$

where  $k_B$  is the Boltzmann constant,  $T$  is the UCST, and  $\beta_T$  is the isothermal compressibility.  $V$  represents the average segment volume for the mixture, and  $\Delta V$  is the difference in volumes between the normal and perdeuterated (undiluted) segments. On the basis of the symmetric version of the Flory-Huggins approximation to the mixing free energy,<sup>3</sup> the critical degree of polymerization is given by

$$N_c = 2/\chi \quad (2)$$

where  $\chi$  is commonly referred to as the "segment-segment interaction parameter". We therefore expect all mixtures of normal and perdeuterated polymers to exhibit a small positive interaction parameter,  $\chi \sim T^{-1}$ , since such isotopic substitution produces changes in molecular volume in essentially all organic compounds.<sup>4</sup> In this communication we report our initial findings concerning the phase behavior of amorphous mixtures of perdeuterated and normal atactic polystyrenes. These results are consistent with our expectation of a universal isotope effect in amorphous polymers.

Monodisperse atactic (anionic) polystyrenes were obtained from Pressure Chemical Co.; the degrees of polymerization and polydispersity indices, as reported by the supplier, are listed in Table I. Binary mixtures ( $\approx 0.1$ -